

Dissolution kinetics of calcite in the H₂O-CO₂ system along the steam saturation curve to 210°C

S. J. TALMAN¹, B. WIWCHAR², W. D. GUNTER² and C. M. SCARFE[†]

¹ C. M. Scarfe Laboratory of Experimental Petrology, Department of Geology, University of Alberta, Edmonton, Alberta, T6H 2G2 Canada

² Alberta Research Council, Oil Sands and Hydrocarbon Recovery Department, P.O. Box 8330, Postal Station F, Edmonton, Alberta, T6H 5X2 Canada

Abstract—The dissolution kinetics of calcite is well described in aqueous solutions below 100°C, but not at higher temperatures. This work documents dissolution experiments performed using single crystals of calcite in a batch reactor at temperatures between 100 and 210°C and using various stirring rates and CO₂ partial pressures. Aqueous speciation was calculated at the temperature of each experiment based on quench measurements. The dissolution rate was found to be dependent on stirring rate, pH and p_{CO_2} . Our data are fit using the rate law proposed by PLUMMER *et al.* (1978) for calcite dissolution at lower temperatures, specifically,

$$\frac{d\text{Ca}}{dt} = k_1[\text{H}^+] + k_2[\text{H}_2\text{CO}_3^*] + k_3[\text{H}_2\text{O}] - k_4[\text{Ca}^{2+}][\text{HCO}_3^-]$$

where k_1 is dependent on stirring rate, k_4 is a function of CO₂ pressure, the bracketed terms represent aqueous activities and $\text{H}_2\text{CO}_3^* = \text{H}_2\text{CO}_3 + \text{CO}_2(\text{aq})$. The rate constants were determined by fitting the experimental data to an integrated form of the rate equation. The constant k_1 is poorly constrained by our experiments except at 100°C and a stirring rate of 500 RPM where it is 1.6×10^{-5} moles $\text{cm}^{-2} \text{s}^{-1}$. The value of k_2 changes slowly with temperature, apparently having a maximum value of about 10^{-6} moles $\text{cm}^{-2} \text{s}^{-1}$ between 100 and 150°C. Finally, k_3 can be expressed by $\log(k_3) = -1300/T - 5.52$ in agreement with the dependence observed at lower temperatures by PLUMMER *et al.* (1978).

INTRODUCTION

THE ALKALINE EARTH CARBONATES, in particular calcite and dolomite, are common minerals in near surface environments. They are formed in diverse geologic settings, almost always by a reaction between aqueous CO₂ and the alkaline earths. Dissolved CO₂ is an important factor controlling pH in many near surface waters and, consequently, mineral stabilities in these waters. As a consequence, equilibrium solubilities and phase relations of carbonate minerals have been studied extensively at low temperatures (FREAR and JOHNSTON, 1929; MACKENZIE *et al.*, 1983). The kinetics of dissolution and precipitation of calcite have also been studied extensively below 100°C (see PLUMMER *et al.*, 1979; INSKEEP and BLOOM, 1985; MORSE, 1983, for recent reviews). These rate studies used a number of different experimental setups, each chosen to elucidate separate aspects of the dissolution reaction. In the simple Ca-CO₂-H₂O system at temperatures below 80°C, calcite dissolution kinetics has been found to be dependent on pH, p_{CO_2} and on the transport conditions in the reaction vessel (PLUMMER *et al.*, 1978; HERMAN, 1982; RICKARD and

SJÖBERG, 1983; COMPTON and DALY, 1984). In more complex aqueous systems, the reaction kinetics can be affected by a number of other aqueous species; effects have been demonstrated with phosphate, sulphate and a host of divalent metals (MORSE, 1983). A number of rate laws have been used to interpret the kinetic data; HOUSE (1981), MORSE (1983) and COMPTON and DALY (1987) discuss the relative merits of these equations.

Carbonates are also important in higher temperature environments. They are common gangue minerals in ore deposits (HOLLAND and MALININ, 1979), they can affect porosity during diagenesis (WOOD, 1986) and they can be used as CO₂ barometers (PERKINS and GUNTER, 1989). HOLLAND and MALININ (1979) reviewed calcite solubility studies in subcritical solutions, and calcite's solubility in supercritical fluids was determined by SHARP and KENNEDY (1965) and FEIN and WALTHER (1987). The incentive for studying the high temperature kinetics of carbonates has been lacking, because most of the traditional applications assume equilibrium. However, kinetic considerations may become important when the relative reaction rates of two minerals are similar, as in the case of carbonate diagenesis, or when a solution is subjected to conditions which change more rapidly than mineral equilibria

[†] Deceased 20 July, 1988.

Table 1. Chemical analysis of Iceland spar (Chihuahua, Mexico)

Element	Concentration (ppm)	Element	Concentration (ppm)
Li	<1.	Mn	<1.
Na	25.	Fe	24.
K	<3.	Al	<6.
Mg	106.	Si	39.
Sr	37.	B	<1.
Ba	<1.	S	<3.
P	22.		

can be established (*e.g.* mid-ocean ridges). Kinetic data at higher temperatures are needed if computer simulations of mid-ocean ridge processes (*e.g.* BOWERS and TAYLOR, 1985) are to be improved. Industrial processes are, generally, much more rapid than geological processes, and consequently the rate data are applicable to models of these processes at most temperatures. Until recently, there were very few kinetic data on any minerals under hydrothermal conditions; however, rates are now available for a number of minerals (quartz—RIMSTIDT and BARNES, 1980; BIRD *et al.*, 1986; feldspars—LAGACHE, 1976; fluorite—POSEY-DOWTY *et al.*, 1986; also HELGESON *et al.*, 1984; WOOD and WALTHER, 1983). Rate data are virtually non-existent for the carbonate system in solutions above 80°C. In this paper we report results on the dissolution kinetics of calcite at temperatures between 100 and 210°C and at steam saturation pressures.

EXPERIMENTAL DESIGN

Optical quality cleavage rhombs of Iceland spar weighing between about 1 and 13 grams from Chihuahua, Mexico (Wards Chemical of Rochester, New York) were lightly etched in dilute HCl to clean the surfaces. A sample was dissolved in nitric acid. The resulting solution was analysed by ICP and the composition of the calcite was calculated (Table 1). Magnesium, at about 100 ppm, was the principal impurity. The surface areas of the calcite crystals (between one and four cm²/g) were below the sensitivity of the BET method. The surface area was calculated from the rhomb geometry, assuming the crystal was a perfect calcite rhombohedron with angles of 75 and 105 degrees. The calculation requires that the crystal is flat; to check this assumption, calcite crystals were examined by SEM (Fig. 1). Three samples were chosen: a freshly fractured crystal, a crystal that was fractured and subsequently etched in 0.01 N HCl for five minutes, and a crystal that had been used in a dissolution experiment. The fractured surfaces show some surface roughness which disappears upon etching of the crystal. The surface of the dissolution experiment crystal appears unchanged from the etched crystal, with the exception of contamination by dust particles. A freshly cleaved surface was also examined on a Dektak II profilometer. Line profile scans of the crystal were made over

several horizontal distances to see if the surface roughness varies with resolution. A typical tracing is shown in Fig. 2. The average slope at each scan length is approximately

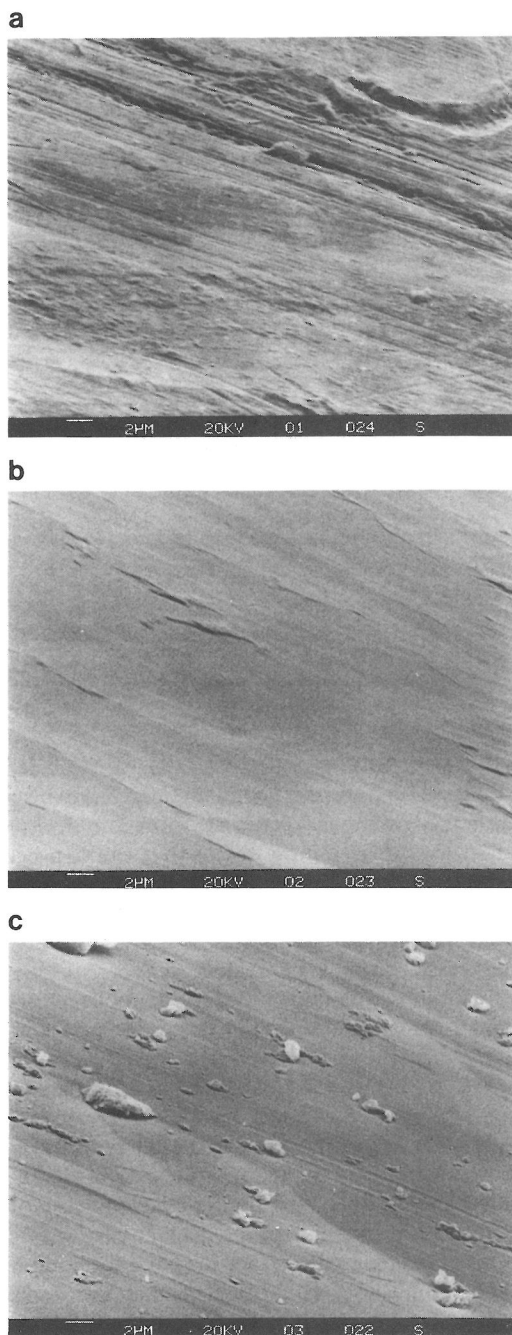


FIG. 1. Scanning electron photomicrograph of Iceland Spar used in dissolution studies a. freshly fractured surface, b. etched in 0.01 N HCl for 5 minutes, c. following a dissolution run. The scale bar in the lower left corner represents 2 μm .

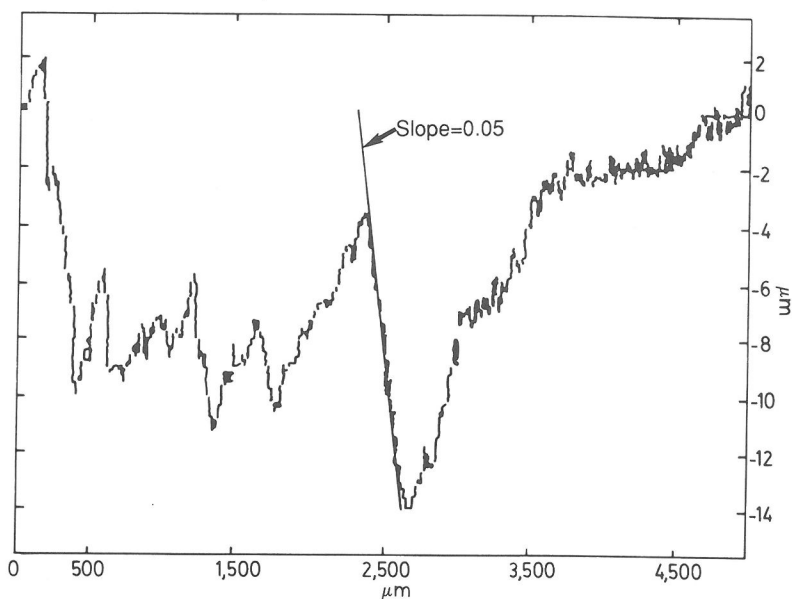


FIG. 2. Line profile scans of Iceland Spar used in kinetic experiments using a Dektak II profilometer. A typical tangent to the surface and its slope are shown. Note the difference in the horizontal and vertical scales.

0.05 from the horizontal. The greatest slope seen was 0.1. If the surface of the crystal were composed of peaks and valleys bounded by planes of slope 0.1, the surface area would only be increased by 1% compared to a perfectly flat surface; therefore, no corrections for surface roughness need be considered. The dimensions of each crystal were measured using vernier calipers.

Reactor design is important in kinetic studies (LEVENSPIEL, 1972; RIMSTIDT and DOVE, 1986; POSEY-DOWTY *et al.*, 1986). We used a stirred batch reactor since it allows the solution and the solid are simply left to react while the solution composition is monitored. Open system experiments on calcite were pioneered by MORSE (1974) who used a "pH-stat" reactor where the system is open to CO_2 and H^+ but not to calcium. PLUMMER *et al.* (1978) used a pH-stat reactor to study calcite dissolution kinetics far removed from equilibrium.

The rate of dissolution is measured directly in open systems (CHOU and WOLLAST, 1984). A number of difficulties arise with open reactors as the temperature of the system is increased. The pH-stat method cannot be used because of the absence of reliable high temperature pH electrodes. Other open systems are complicated by the need for precise determination of the chemical composition of quench samples. The reaction rate is determined by the difference in the composition of the input and output solutions, which makes the rate determination very sensitive to analytic error. The number of steps required to treat the quench samples leads to relatively large uncertainties in the solution composition.

In order to obtain the dissolution rate from a closed reactor, the solution data must be differentiated; errors associated with derived quantities are generally greater than those of the original data. However, if a rate law is postulated, its validity can be checked with the data from a single batch reactor run, since each experiment provides rate data for variable solution compositions. Since a number of rate laws have been proposed for calcite at lower temperatures, we can test our data against these to see if they are applicable. For these reasons, a closed batch reactor was used for all the experiments reported here.

The experiments were performed in a four litre Parr stirred stainless steel autoclave; a schematic diagram of the apparatus is shown in Fig. 3. Impellers affect stirring in both the gas and liquid phases. Two types of crystal holder were used. Initial runs used a cage holder that surrounded the crystal, and consequently restricted the circulation of the solution near the crystal. Later runs used a holder consisting of two strands of stainless steel wire which reduces the interference with the fluid flow near the sample. A screw device allows the crystal to be raised or lowered while the autoclave is at pressure. The autoclave was precharged with CO_2 and 2.0 kg of deionized water were added. Run conditions were achieved while the crystal was in the vapour. At the start of a dissolution experiment, the crystal was lowered into the aqueous phase. Samples of the solution (50 ml) in the autoclave were taken regularly through floating piston sample tubes. The floating piston ensures that there is no great pressure drop at the dip tube where the sample is removed from the autoclave, and hence no boiling. The solution removed during sampling was replaced by a solution whose CO_2 pressure was near to the starting composition of the autoclave solution. The temperature was maintained at the run temperature $\pm 0.2^\circ\text{C}$,

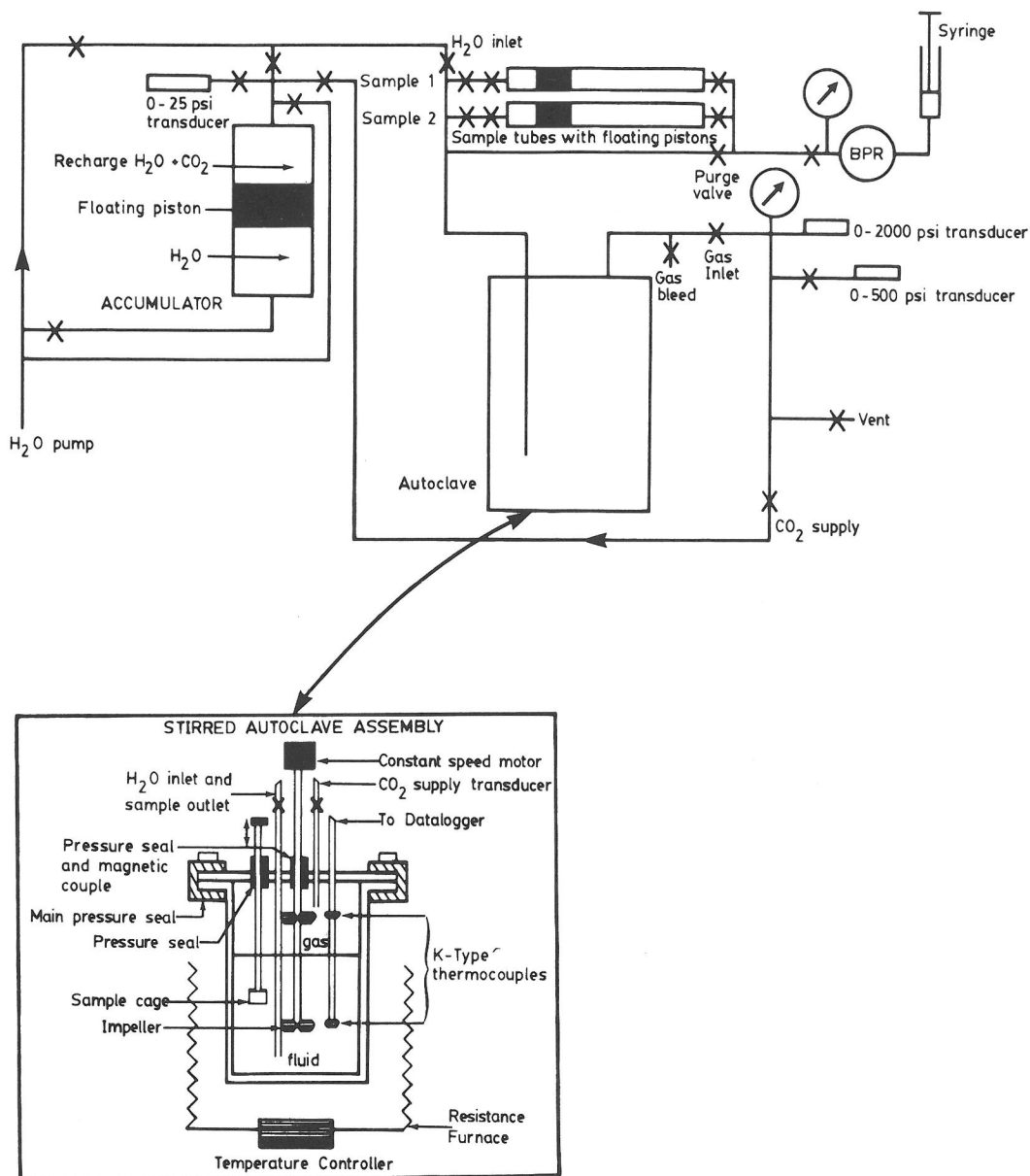


FIG. 3. Schematic diagram of the stirred autoclave system used in the experiments. The back pressure regulator is labeled BPR.

except immediately after sampling, when the temperature would drop by about 2°C.

The concentration of carbonic acid at run conditions could not be calculated from the initial charge of CO₂ since a small thermal gradient in the vapour made the partitioning of CO₂ difficult to predict. Consequently two samples were taken at each time interval. One sample was basified with NaOH to keep the CO₂ in solution and was analysed for TIC (total inorganic carbon). The other sample was split. One portion was acidified and analysed for cations by ICP and the pH and TIC were measured on the other portion after it had stabilized with respect to loss of

CO₂. The difference in TIC between the two samples represented the CO₂ lost from the unbasified quench sample.

EXPERIMENTAL RESULTS AND DATA REDUCTION

Dissolution experiments were performed at 210, 150, and 100°C and a variety of stirring rates and CO₂ pressures (Table 2 and Appendix). Plots of calcium vs. elapsed time for these experiments are shown in Fig. 4. The equations used to generate the

Table 2. Summary of experimental conditions*

Experiment	Temp °C	Initial TIC (mmoles/kg)	Stirring rate (rpm)	Surface area (cm ²)	Crystal mass (g)	Remarks
W130587	210	31.	500	4.35	1.014	crystal 1
W150987	210	38.	750	3.99	0.895	crystal 1
W271087	210	39.	750	3.80	0.774	crystal 1
W011287	210	32.	300	3.6**	0.654	crystal 1
W150288	210	36.	500	4.61	1.518	crystal 2
W250288	210	100.	500	4.40	1.396	crystal 2
W140388	210	39.	500	2.88	0.417	crystal 1
W160588	210	5.0	500	4.09	1.208	crystal 2
W310588	210	38.	750	3.92	1.145	crystal 2
W251088	150	7.1	500	17.5	13.243	crystal 3
W141288	150	7.3	350	17.5	13.042	crystal 3
W020389	100	0.	500	17.5	12.848	crystal 3
W200389	100	16.5	500	17.4	12.790	crystal 3
W040489	100	0.	500	17.3	12.230	crystal 3
						0.002 molal HCl

* Runs W130587 and W150987 used cage crystal holder, all other runs used wire holder. Solution mass 2.0 kg for all the runs.

** Estimated.

curves will be discussed later. As expected, the aqueous calcium concentration increases steadily with time, reaching a maximum value when equilibrium is approached.

The total calcium and carbon in the solution were used to calculate the distribution of species and the saturation quotient ($\Omega = [\text{Ca}^{2+}][\text{CO}_3^{2-}]/K_{sp}$) at run conditions. The calculation involves solving the mass balance equations for Ca and TIC, subject to mass action and charge balance constraints. The stability constants for the aqueous complexes and the solubility product of calcite were taken from the SOLMINEQ.88 data base (KHARAKA *et al.*, 1988; Table 3). The stability of the complex CaHCO_3^+ was reduced from the value in the SOLMINEQ.88 data base. If this stability constant was not decreased, the calculated speciation was still considerably undersaturated with respect to calcite at the end of the experimental run. This suggests that this complex is not stable in dilute solutions at hydrothermal temperatures. PLUMMER and BUSENBERG (1982) present low temperature solubility data of calcium carbonates that are consistent with a lower stability constant for this complex than is in the SOLMINEQ.88 data base. FEIN and WALTHER (1987) reached a similar conclusion for supercritical $\text{H}_2\text{O}-\text{CO}_2$ solutions. Values of the ion activity product $Q (=K_{sp}\Omega)$ at saturation for the 210°C runs varied between 2.7×10^{-12} and 3.8×10^{-12} , and were, on average only slightly higher (3.3×10^{-12}) than the value of K_{sp} in the SOLMINEQ.88 data base of 2.9×10^{-12} . Furthermore, data

from some initial runs (not discussed here) supports this value for K_{sp} . Initial runs were performed without replacing the solution lost from the system during sampling. As a consequence, the solution was depleted in CO_2 through the run, which lead to calcite precipitation late in the run. In one run dissolved calcium and TIC decreased by 7% and 25% respectively; however, Q maintained a near constant value between the previously mentioned limits. This suggests that the value of K_{sp} used here is reasonable.

An alternative method was used in some runs to check the calculated solution composition. This involved using Ca, pH and TIC from the quenched sample. The speciation was calculated with these data and then an amount of CO_2 was titrated back into the sample to make up the difference between the TIC from the basic sample and the quenched sample. The two sets of calculations were generally in agreement. However, since this calculation uses all the same data as the first calculation, as well as the pH of the quench sample and the TIC of the acidic sample we chose, in later experiments, to use only the first calculation of the solution chemistry at run conditions. A possible error in the calculation arises from the failure to consider any cations other than calcium in a charge balanced solution; however, calcium was the dominant cation in virtually all of the samples. Some of the initial samples had relatively high iron contents (see Appendix) which quickly plated out on the autoclave.

A number of empirical rate laws have been used to fit calcite dissolution data in aqueous solutions

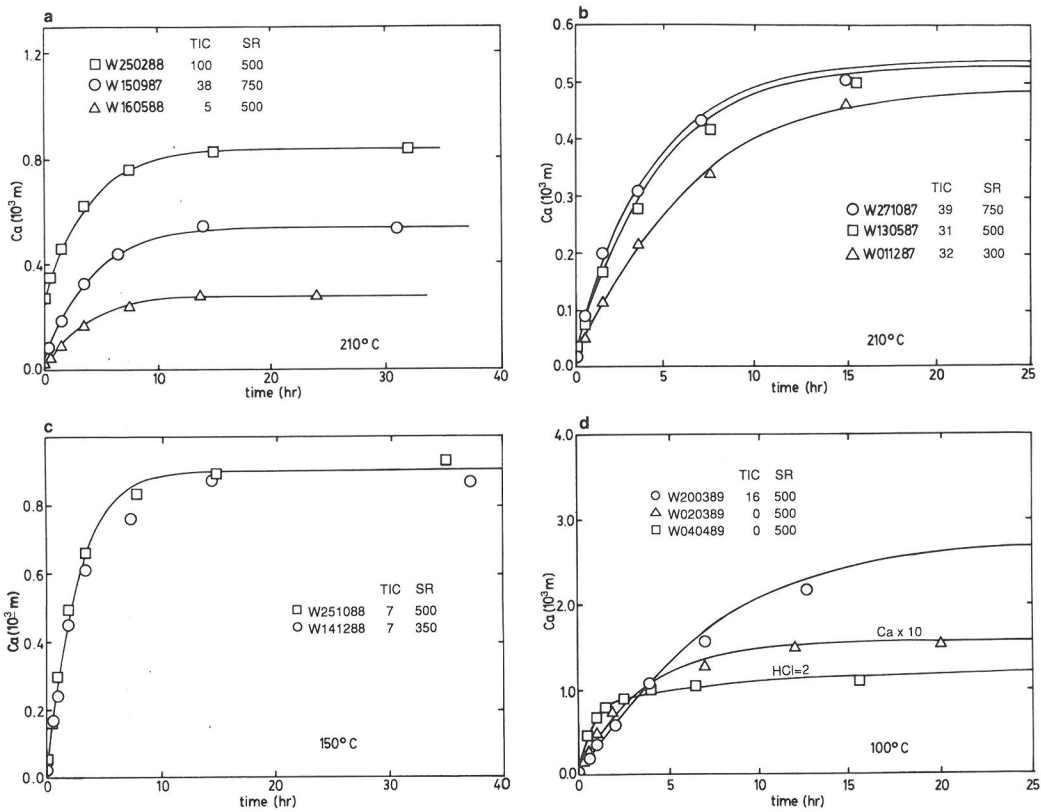


FIG. 4. Aqueous calcium concentration (millimoles/kg) versus elapsed time in hours for dissolution experiments at 100, 150 and 210°C. Curves were fit according to the rate expression of PLUMMER *et al.* (1978) using the rate constants listed in Table 4. The run conditions are shown in the figure, stirring rate is abbreviated as SR and concentration units of TIC and HCl are millimoles/kg. The run conditions are also listed in Table 2.

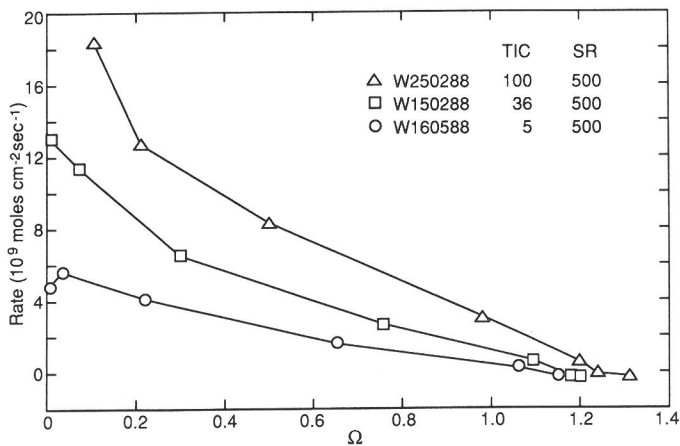


FIG. 5. Dissolution rate (in nanomoles $\text{cm}^{-2} \text{s}^{-1}$) plotted against Ω for three runs at various values of p_{CO_2} at a constant stirring rate (SR).

(see MORSE, 1983). Most of the rate laws are based on Ω , and are of the form:

$$\text{Rate} = k(1 - \Omega)^n$$

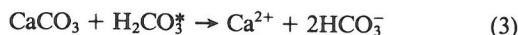
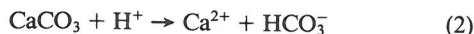
where n and m are fit parameters. To test this rate law, the reaction rate was determined by numerically differentiating the calcium concentration vs. time curve using a second degree interpolating polynomial. The rate was plotted in Fig. 5 as a function of Ω for runs at 210°C and three different p_{CO_2} 's. Errors associated with the calculated initial rate are about 10%. The uncertainty in Ω is large; as discussed earlier the average value of the solubility product calculated here is 15% greater than the value of K_{sp} used to calculate Ω . As well, since the value of $[\text{CO}_3^{2-}]$ is calculated from a charge balance equation it is sensitive to errors in $[\text{Ca}^{2+}]$ which leads to an error of $\pm 15\%$. The apparent dissolution of calcite in supersaturated solutions is a consequence of these errors. Although the errors are relatively large, it is clear that there are differences in the reaction rate. All the data should plot along the same curve if the rate is solely dependent on Ω . Clearly, this is not the case; therefore, any rate law simply based on Ω is inadequate. Fig. 5 demonstrates a dependence of the rate on p_{CO_2} which cannot be described solely in terms of Ω .

The stirring rate dependence of the rate of calcite dissolution is well documented (LUND *et al.*, 1975; PLUMMER *et al.*, 1978; 1979; COMPTON and DALY, 1984) and it has been demonstrated that in acidic solution it is the rate of transport of H^+ to the surface that limits the reaction. Stirring rate dependence can be seen in our data (Fig. 4b). This figure shows the calcium concentration as a function of time for three runs performed at similar p_{CO_2} 's. The upper curve was obtained using a slightly smaller crystal than the middle curve and a higher stirring rate (runs W130587 and W271087). The separation of these curves occurs early in the run, indicating that the stirring rate dependence is due to hydronium transport. The lower curve is from run W11287 at a still lower stirring rate; however, the crystal was smaller still.

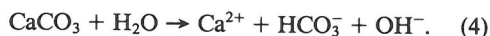
To our knowledge PLUMMER *et al.* (1978) are the only investigators who have tried to separate the effects of both p_{CO_2} and H^+ on the rate. Their rate expression is

$$\frac{d\text{Ca}}{dt} = k_1[\text{H}^+] + k_2[\text{H}_2\text{CO}_3^*] + k_3[\text{H}_2\text{O}] - k_4[\text{Ca}^{2+}][\text{HCO}_3^-] \quad (1)$$

where k_1 - k_3 and k_4 are rate constants and the bracketed terms represent the activities of these species in the solution. This rate law is developed by assuming that calcite dissolution proceeds by three simultaneous reactions:



and



PLUMMER *et al.* (1978; 1979) derive Equation 1 from a mechanistic model of dissolution. The forward rate of reaction (2), $k_1[\text{H}^+]$, is limited by the rate of transport to the calcite surface, so that k_1 is dependent on stirring rate. As the stirring rate is increased, k_1 should increase until it reaches $K_{eq,1}/k_{-1}$ where $K_{eq,1}$ is the equilibrium constant for reaction 2, and k_{-1} is the rate constant for the back reaction. PLUMMER *et al.* (1978) grouped the rate for all three back reactions into one term involving k_4 ; however, in order to do this they had to introduce a p_{CO_2} dependence into k_4 . Although this is not necessary since the forward and backward rate constants for elementary reactions are related to the equilibrium constant (see LASAGA, 1981), it is convenient for fitting our experimental data.

DETERMINATION OF RATE CONSTANTS

The speciation calculated by the methods described previously can be used to calculate rate constants for the Plummer rate expression. Extracting the forward rate constants for reactions 2, 3 and 4 from the batch reactor data requires either integrating the proposed rate expression or numerically differentiating the experimentally determined concentration evolution. We chose to integrate an approximation to the rate law rather than the numerical differentiation. The rate obtained by differentiation is very sensitive to errors in the solution analysis.

The complexity of the rate law requires that a simplification be introduced in order to make the expression integrable. The activity of the aqueous species in (1) (except Ca^{2+}) at any time, t , between sampling times t_1 and t_2 was estimated by a linear extrapolation of their activity, so that the various activity terms in Equation (1) can be written

$$a_i(t) = \frac{a_i(t_2) - a_i(t_1)}{t_2 - t_1} (t - t_1) + a_i(t_1), \quad (5)$$

Table 3. Values of thermodynamic constants used in the calculations. K_1 and K_2 are the first and second dissociation constants of carbonic acid, K_w is the dissociation constant of water, and K_{CaCO_3} is the dissociation constant for $CaCO_3$. The stability constant for $CaHCO_3^+$ was set to -1.0 for all temperatures

T	$\log K_1$	$\log K_2$	$\log K_w$	$\log K_{CaCO_3}$	$\log K_{sp}$	B^*
100.	-6.43	-10.16	-12.26	-4.17	-9.27	0.046
150.	-6.77	-10.39	-11.64	-4.67	-10.16	0.047
210.	-7.30	-10.87	-11.20	-5.60	-11.53	0.045

where a_i is the activity of species i and $t_1 < t < t_2$. In this case Equation (1) becomes

$$rate = \frac{M}{A} \frac{dCa}{dt} = (C_1 + D_1 t)Ca + C_2 + D_2 t \quad (6)$$

where Ca is the concentration (molal) of calcium in solution, A and M are the surface area of the crystal and the solution mass respectively and

$$C_1 = k_4 \left[f_{Ca}(t_1)[HCO_3^-(t_1)] - \frac{f_{Ca}(t_2)[HCO_3^-(t_2)] - f_{Ca}(t_1)[HCO_3^-(t_1)]}{t_2 - t_1} t_1 \right]$$

$$D_1 = k_4 \left[\frac{f_{Ca}(t_2)[HCO_3^-(t_2)] - f_{Ca}(t_1)[HCO_3^-(t_1)]}{t_2 - t_1} \right]$$

$$C_2 = k_1 \left[[H^+(t_1)] - \frac{[H^+(t_2)] - [H^+(t_1)]}{t_2 - t_1} t_1 \right] + k_2 \left[[H_2CO_3^*(t_1)] - \frac{[H_2CO_3^*(t_2)] - [H_2CO_3^*(t_1)]}{t_2 - t_1} t_1 \right] + k_3 \left[[H_2O(t_1)] - \frac{[H_2O(t_2)] - [H_2O(t_1)]}{t_2 - t_1} t_1 \right]$$

and

$$D_2 = k_1 \frac{[H^+(t_2)] - [H^+(t_1)]}{t_2 - t_1} + k_2 \frac{[H_2CO_3^*(t_2)] - [H_2CO_3^*(t_1)]}{t_2 - t_1} + k_3 \frac{[H_2O(t_2)] - [H_2O(t_1)]}{t_2 - t_1}$$

and f_{Ca} relates Ca to $[Ca^{2+}]$ and it is assumed to be the same for the fit and experimentally determined calcium concentration. Despite the approximations

made in integrating the rate expression, it should be more accurate than the alternative approach of differentiating the concentration data, since it uses requires one less calculated quantity (dCa/dt).

Activity coefficients, γ_i were calculated using the expression

$$\log \gamma_i = \frac{-A(T)Z_i^2\sqrt{I}}{1 + \bar{a}_i(T)B(T)\sqrt{I}} + B^*(T)I$$

(HELGESON, 1969), where I is the ionic strength, Z_i is the ionic charge, and \bar{a} is an ion size parameter. A and B are related to the density, ρ , and dielectric constant, ϵ of water by

$$A = \frac{1.82 \times 10^6 \sqrt{\rho}}{(\epsilon T)^{3/2}}$$

and

$$B = \frac{50.3 \times 10^8 \sqrt{\rho}}{\sqrt{\epsilon T}}$$

(HELGESON, 1969) and B^* is listed in Table 3. The contribution of the B^* term to the activity coefficient is small for all the samples. Based upon the linear approximation, Equation 1 can be integrated to give

$$Ca(t) = \exp\left[-\frac{D_1}{2}(t_1^2 - t^2)\right] + C_1(t_1 - t) \left[Ca(t_1) - \frac{D_2}{D_1} \right] + \frac{D_2}{D_1} + \sqrt{\frac{2}{D_1}} \left(C_2 - \frac{D_2 C_1}{D_1} \right) \times \left[\text{Daw} \left(\sqrt{\frac{D_1}{2}} t + \frac{C_1}{\sqrt{2D_1}} \right) - \exp\left[-\frac{D_1}{2}(t_1^2 - t^2) + C_1(t_1 - t)\right] \times \text{Daw} \left(\sqrt{\frac{D_1}{2}} t_1 + \frac{C_1}{\sqrt{2D_1}} \right) \right] \quad (7)$$

where Daw refers to the Dawson integral

$$\text{Daw}(x) = \exp(-x^2) \int_0^x \exp(y^2) dy. \quad (8)$$

Equation 7 relates the concentration of calcium at time t_{i+1} to the concentration at time t_i (and, by recursion, to its initial concentration) and the activities of the other species appearing in (1). It is linear in C_2 and D_2 and non-linear in C_1 and D_1 , and therefore, it is linear in the three constants k_1 – k_3 and non-linear in k_4 . Consequently, given a k_4 , values of k_1 – k_3 which minimize the expression $\sum_i (Ca(t_i)' - Ca(t_i))^2$, where $Ca(t_i)'$ is the value from

(7), can be determined. A number of values for k_4 were tried in order to obtain the one which gave lowest deviation from the data. It is also possible to fit the entire curve with an additional constant, $[Ca(0)]$; however, with the approximations already made, it is unlikely to provide a superior fit. Values of k_1 and k_4 were in fair agreement for different runs at the same stirring rate and p_{CO_2} ; however, values of k_2 and k_3 were not consistent. This is because neither $[H_2O]$ nor $[H_2CO_3^*]$ change very much during a given run, so these parameters are very sensitive to small changes in $[H_2CO_3^*]$ through the run (or random errors in the TIC data). However, the sum $(k_3 + k_2[H_2CO_3^*])$ is relatively insensitive. Therefore, the values for k_2 and k_3 were determined from pairs of experiments at different carbonic acid activities ($[H_2CO_3^*]_{(1)}$ and $[H_2CO_3^*]_{(2)}$). The net contribution to the rate by water and carbonic acid $(k_3 + k_2[H_2CO_3^*])$ should be the same with the new constants k_2 and k_3 as with the calculated values $k_{2,(1)}$, $k_{3,(1)}$, associated with $[H_2CO_3^*]_{(1)}$ and $k_{2,(2)}$ and $k_{3,(2)}$ associated with $[H_2CO_3^*]_{(2)}$, so that

$$k_3 + k_2[H_2CO_3^*]_{(1)} = k_{3,(1)} + k_{2,(1)}[H_2CO_3^*]_{(1)}$$

and

$$k_3 + k_2[H_2CO_3^*]_{(2)} = k_{3,(2)} + k_{2,(2)}[H_2CO_3^*]_{(2)}$$

These equations are solved for k_2 and k_3 . Fig. 4a demonstrates that the values calculated in this manner are consistent with rate data from a run at a third p_{CO_2} . The constant k_4 can be calculated given values of k_1 , k_2 , k_3 and p_{CO_2} using the relation given by PLUMMER *et al.* (1978) which becomes, after taking into consideration several assumptions which they discuss,

$$k_4 = \frac{K_2}{K_{sp}} \left(k'_1 + \frac{1}{a_{H_3O^+}} [k_2 a_{H_2CO_3^*} + k_3 a_{H_2O}] \right) \quad (9)$$

where K_2 is the second dissociation constant of carbonic acid, k'_1 is the limiting value of k_1 at infinite stirring rate, and $a_{H_3O^+}$ is the activity of hydronium at the crystal surface. This can be approximated by

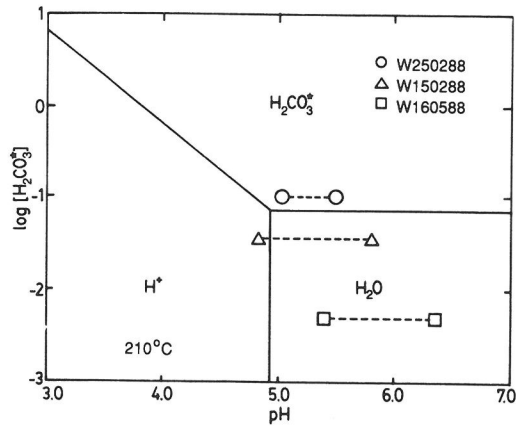


FIG. 6. The initial and final solution hydronium and $H_2CO_3^*$ activities from three runs at 210°C and different p_{CO_2} 's are shown in this figure connected by dashed lines. The solid lines divide the plot into regions where each of the three forward reactions make the dominant contribution to the net forward rate at this temperature. Reaction between the crystal and condensate is responsible for the relatively high initial pH in the experiment at high p_{CO_2} .

the equilibrium value of H^+ in the system, and its value is generally sufficiently small to ensure that k'_1 is negligible compared to the second term in the parentheses.

Fig. 6 shows the solution compositions where the contributions from each of the three forward reactions are dominant at 210°C. The values of the rate constants used to develop this plot and Fig. 4 are given in Table 4. The initial and final solution compositions of three runs at different p_{CO_2} 's are also shown in Fig. 6. Each of the three rate terms predominate for at least a portion of one of the runs. The confidence in the estimates of the rate constants is roughly related to the number of data points in each area; the rate constant, k_1 is the least well defined.

Table 4. Comparison of the results of this work with values extrapolated from the Arrhenius fit given by PLUMMER *et al.* (1978). These equations are $\log k_1^{ext} = -2.802 - 444/T$; $\log k_2^{ext} = -0.16 - 2177/T$, and $\log k_3^{ext} = -4.10 - 1737/T$

T	Rate constants (moles $cm^{-2} s^{-1}$)					
	This work			Extrapolated		
	$\log k_1$	$\log k_2$	$\log k_3$	$\log k_1^{ext}$	$\log k_2^{ext}$	$\log k_3^{ext}$
100.	-4.8	-6.3	-9.0	-4.0	-6.0	-8.8
150.	-4.1	-6.2	-8.6	-3.9	-5.3	-8.2
210.	-3.3	-7.1	-8.2	-3.7	-4.7	-7.7

A single experiment was performed at 100°C in a starting solution with $2. \times 10^{-3}$ molal HCl, which defines the value of k_1 very well at the run conditions. This experiment could not be performed at other temperatures due to the corrosive nature of the initial solutions. We are in the process of obtaining lined autoclaves in which these experiments can be performed. This will help to define k_1 with more certainty. The values of k_1 in Table 4 are based on data obtained at a stirring rate of 500 RPM. The values of $\log(k_1)$ used to generate the upper and lower curves in Fig. 4b differ from the value in Table 4 by 0.15 and -0.58 respectively.

The rate constants and the rate expression were used to simulate the dissolution reaction. The calculations require as input the initial Ca and, for those runs with an applied p_{CO_2} , the total dissolved carbonate in solution (essentially constant through

the run). The total carbonate in the runs without an applied p_{CO_2} changed appreciably through the run, so a temperature dependent parameter, β (the ratio of H_2CO_3^* in solution to the mass of CO_2 in the vapour), was introduced to simulate the partitioning of CO_2 between the solution and vapour, and a mass balance on carbonate was included in the calculations. A value of β which fit the measured TIC values was determined. The data input defines the initial solution speciation and, from Equation (1), the initial rate of calcite dissolution. This rate is used to determine how much calcium will be added to the solution during a given time interval, after which the solution composition and dissolution rate are recalculated. This is repeated until the solution becomes saturated. The curves plotted on Fig. 4 are calculated in this manner. The agreement between these curves and the data is very good, with

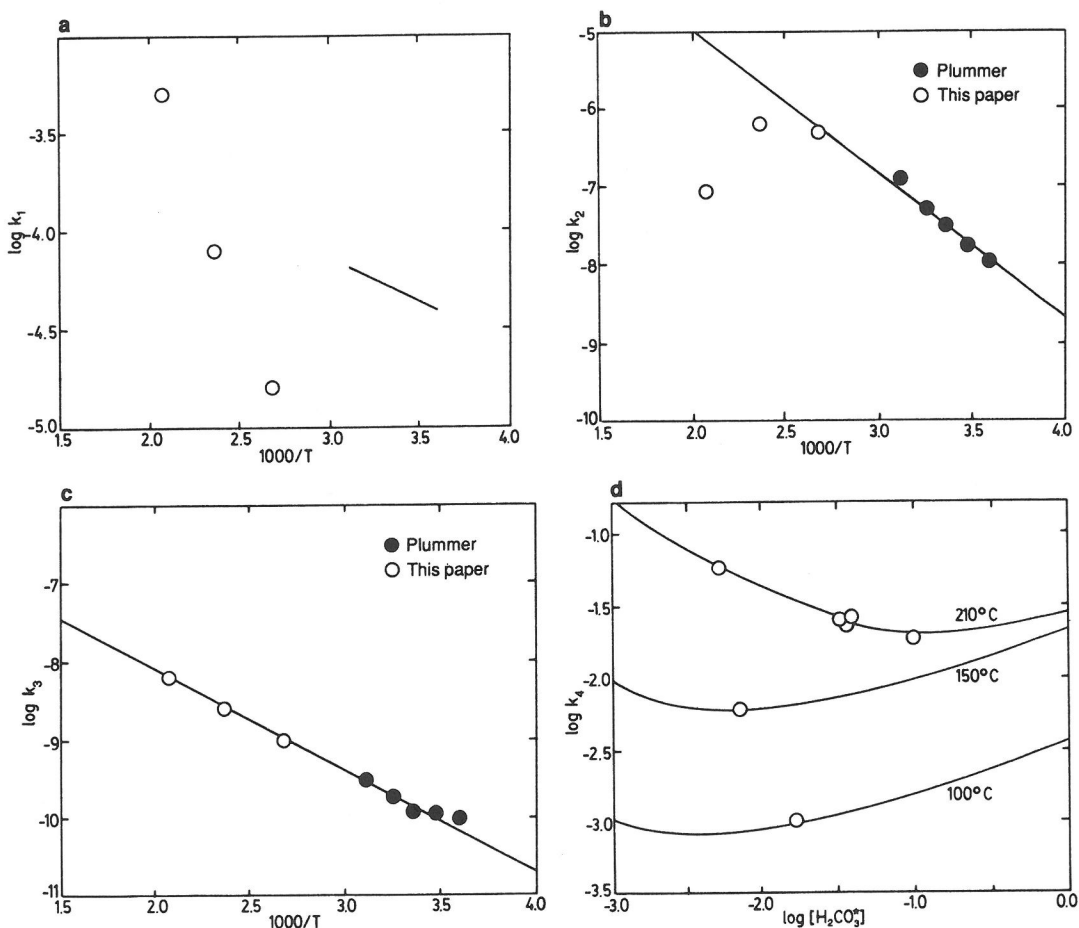


FIG. 7. Arrhenius plots of the rate constants k_1 , k_2 and k_3 (in moles $\text{cm}^{-2} \text{s}^{-1}$) are shown in figures 7a, 7b, and 7c with Plummer's rate constants from 5 to 60°C and our rate constants at 100, 150, and 210°C. Figure 7d shows the fit values of k_4 from several runs. The curves show the values of k_4 predicted by Equation 9.

the exception of some intermediate points in the two lower temperature runs; however, the fit in the region where the rate of the back reaction is small is much better. The discrepancy between the predicted and fit values may be due to an incorrect expression for the back reaction. COMPTON and DALY (1987) performed calcite dissolution experiments in a batch reactor. The fit of their data to Equation 1 showed a similar discrepancy in intermediate saturations. BUSENBERG and PLUMMER (1986) and CHOU *et al.* (1989) use a rate expression very similar to Equation (1) to describe the rate of dissolution of a number of single component carbonates, but with different expressions for the back reactions.

TEMPERATURE DEPENDENCE

PLUMMER *et al.* (1978) studied calcite dissolution kinetics as a function of solution composition for temperatures between 0 and 60°C. They fit the temperature dependence of the rate constants with an Arrhenius relationship,

$$\log k = a - \frac{b}{T} \quad (10)$$

where T is the temperature in K. The values of a and b determined by PLUMMER *et al.* (1978) are given in Table 4, along with the extrapolated rate constants. The rate constants calculated here are shown on an Arrhenius plot in Fig. 7, together with the temperature dependence determined by PLUMMER *et al.* (1978). Errors on the 210°C points were estimated by a Monte-Carlo type calculation in which the initial calcium and TIC values were varied by a random errors of less than 5%. Two of the rate constants k_1 , k_2 , and k_3 were held constant while the third constant and k_4 were determined using the regression calculation described previously. After about fifty calculations the mean and standard deviation of the k values were calculated. The standard deviations determined in this way were generally within 15% of the mean.

The logarithms of our rate constants k_2 and k_3 at 100°C are about 0.25 lower than the extrapolated values; this discrepancy is consistent with errors in surface area estimates or differences in defect densities (SCHOTT *et al.*, 1989; CHOU *et al.*, 1989). CHOU *et al.* (1989) also found discrepancies between their calcite dissolution rate data and those predicted using rate constants given by PLUMMER *et al.* (1978) of a similar magnitude. The expression by PLUMMER *et al.* (1978) for k_3 above 25° extrapolates relatively well to our values; however, the behavior of k_1 and k_2 with temperature is more complex. The

value of k_2 at 100°C is essentially co-linear with the low temperature data; however, the slope of the curve decreases as the temperature increases to such an extent that the slope of the curve is negative at 210°. The values of k_1 obtained here show an irregular behaviour with temperature. For reasons described above, the value of k_1 is the least well defined by our experiments, with the exception of the 100° datum. This value is considerably lower than the value fit from the low temperature data, even if it is increased by a factor of two on the assumption that there is discrepancy due to surface area or crystal features. PLUMMER *et al.* (1978) observed variations in the value of k_1 by a factor of about 1.5 by changing the stirring rate. Our runs were done at a lower stirring rate, but, perhaps more importantly, on a much bigger crystal. Flow across the larger crystal surface will be less turbulent than for the smaller grains used in the low temperature studies. Until it is possible to perform the higher temperature experiments in more acidic solutions, it will be difficult to define k_1 . However, the data we have (Fig. 7a) suggests that the rate increases with temperature more rapidly than was observed by PLUMMER *et al.* (1978). It is difficult to assign any significance to this observation, since the values are not very well defined and there are additional complications associated with the stirring rate dependence. Fig. 7d plots the values of k_4 determined here along with the values calculated from Equation 9 at the three run temperatures.

The apparent negative activation energy of k_2 at temperatures above 150°C can most easily be explained by invoking a change in reaction mechanism. A very slight decrease could be attributed to a decrease in the equilibrium constant for the hydration of CO₂(aq) with temperature (PALMER and VAN ELDIK, 1983), but the observed decrease is much greater than can be attributed to this. In addition, the hydration reaction is promoted by an increase in pressure which will decrease the effect. Our data suggests a change in the mechanism of reaction (3) with increased temperature. With only the batch reactor data obtained here, it is difficult to propose, with any confidence, a new reaction mechanism for the reaction between calcite and carbonic acid at these temperatures.

Our data are consistent with the PLUMMER *et al.* (1978) rate equation at 210°, despite the change in mechanism of reaction (3). Their rate equation (Equation 1) will still be valid if the mechanism changes from being controlled by the rate of reaction between H₂CO₃* and the calcite surface, as postulated by PLUMMER *et al.* (1978), to a rate controlled by the decomposition of a surface calcite-carbonic

acid complex. In this case, the rate of dissolution due to reaction with carbonic acid, r_2 , will be $r_2 = k_{sc}K_{eq} [H_2CO_3^*]$ where k_{sc} is the rate of decomposition of the surface complex and K_{eq} is the equilibrium constant for the formation of the surface complex. If the complex is formed by a sufficiently exothermic reaction the apparent activation energy obtained by considering reaction (3) to be rate limiting may be negative.

CONCLUSIONS

The rate of calcite dissolution from ambient to temperatures in excess of 200°C depends on temperature, flow rate, and pressure of CO₂ and is well described by the rate law proposed by PLUMMER *et al.* (1978). The value of k_1 is poorly constrained by our experiments except at 100°C at a stirring rate of 500 RPM where a quantity of acid was added at the start of the experiment. An anomalous temperature dependence is seen in k_2 which shows very little dependence on temperature and appears to have a maximum near 150°C. This is a clear indication of a change in reaction mechanism, although the linear dependence of the rate on $[H_2CO_3^*]$ appears to remain. The rate constant, k_3 , fits well with the extrapolation of PLUMMER *et al.* data above 25°C with an activation energy of about 24.7 kJ mole⁻¹. Further experiments in lined autoclaves are required to more fully understand the behaviour of k_1 with temperature.

Acknowledgements—Financial support for this work was obtained by C. Scarfe (later managed by K. Muehlenbachs) from the Alberta Oil Sands Technology and Research Authority (AOSTRA). L. Holloway, K. Montgomery, and B. Young provided assistance with the chemical analyses. Thanks are also due to Lei Chou for providing us with a preprint of her paper, J. Fein, P. Glynn, N. Plummer and D. Rimstidt for their reviews of the initial manuscript, Karen Jensen for drafting services, M. K. Allen for splicing infinitives, and finally to Jamey Hovey and Ernie Perkins for technical and logistical aid. We are honoured that this paper has been included in this volume.

REFERENCES

- BIRD G., BOON J. and STONE T. (1986) Silica transport during steam injection into oil sands. I. Dissolution and precipitation kinetics of quartz: new results and review of existing data. *Chem. Geol.* **54**, 69–80.
- BOWERS T. S. and TAYLOR H. P. JR. (1985) An integrated chemical and stable-isotope model of the origin of mid-ocean ridge hot spring systems. *J. Geophys. Res.* **90**, 12,583–12,606.
- BUSENBURG E. and PLUMMER L. N. (1986) A comparative study of the dissolution and crystal growth kinetics of calcite and aragonite. In *Studies in Diagenesis* (ed. F. A. MUMPTON), *U.S. Geol. Surv. Bull.* **1578**, pp. 139–168.
- CHOU L. and WOLLAST R. (1984) Study of the weathering of albite at room temperature and pressure with a fluidized bed reactor. *Geochim. Cosmochim. Acta* **48**, 2205–2217.
- CHOU L., GARRELS R. M. and WOLLAST R. (1989) A comparative study of the kinetics and mechanisms of dissolution of carbonate minerals. *Chem. Geol.* (submitted).
- COMPTON R. G. and DALY P. J. (1984) The dissolution kinetics of Iceland spar single crystals. *J. Colloid Interface Sci.* **101**, 159–166.
- COMPTON R. G. and DALY P. J. (1987) The dissolution/precipitation kinetics of calcium carbonate: An assessment of various kinetic equations using a rotating disc method. *J. Colloid Interface Sci.* **115**, 493–498.
- FEIN J. B. and WALTHER J. V. (1987) Calcite solubility in supercritical CO₂-H₂O fluids. *Geochim. Cosmochim. Acta* **51**, 1665–1673.
- FREAR G. L. and JOHNSTON J. (1929) Solubility of calcium carbonate (calcite) in certain aqueous solution at 25°C. *Amer. Chem. Soc. J.* **51**, 2082–2093.
- HELGESON H. C. (1969) Thermodynamics of hydrothermal systems at elevated temperatures and pressures. *Amer. J. Sci.* **267**, 729–804.
- HELGESON H. C., MURPHY W. M. and AAGAARD P. (1984) Thermodynamic and kinetic constraints on reaction rates among minerals and aqueous solutions. II. Rate constants, effective area, and the hydrolysis of feldspar. *Geochim. Cosmochim. Acta* **48**, 2405–2432.
- HERMAN J. S. (1982) The dissolution kinetics of calcite, dolomite and dolomitic rocks in the carbon dioxide-water system. Unpublished PhD. thesis, Pennsylvania State University, 219p.
- HOLLAND H. D. and MALININ S. D. (1979) The solubility and occurrence of non-ore minerals. In *Geochemistry of Hydrothermal Ore Deposits* (ed. H. L. BARNES), Chap. 9, pp. 461–508. John Wiley and Sons.
- HOUSE W. A. (1981) Kinetics of crystallisation of calcite from calcium bicarbonate solutions. *J. Chem. Soc. Faraday Trans. 1* **77**, 341–359.
- INSKEEP W. P. and BLOOM P. R. (1985) An evaluation of rate equations for calcite precipitation kinetics at pCO_2 less than 0.01 atm and pH greater than 8. *Geochim. Cosmochim. Acta* **49**, 2165–2180.
- KHARAKA Y. K., GUNTER W. D., AGGARWAL P. K., PERKINS E. H. and DEBRAAL J. D. (1988) SOLMINEQ.88: A computer program code for geochemical modeling of water-rock interactions. U.S. Geol. Surv. Water-Resources Investigations Report 88-4227.
- LAGACHE M. (1976) New data on the kinetics of the dissolution of alkali feldspar at 200°C in carbon dioxide charged water. *Geochim. Cosmochim. Acta* **40**, 157–161.
- LASAGA A. C. (1981) Rate laws of chemical reactions. In *Kinetics of Geochemical Processes* (eds. A. C. LASAGA and R. J. KIRKPATRICK), Chap. 1, pp. 1–68. *Reviews in Mineralogy*, **8**.
- LEVENSPIEL O. (1972) *Chemical Reaction Engineering*. 2nd ed. John Wiley, 578 pp.
- LUND K., FOGLER H. S. and MCCUNE C. C. (1975) Acidization—II. The dissolution of calcite in hydrochloric acid. *Chem. Eng. Sci.* **30**, 825–835.
- MACKENZIE F. T., BISCHOFF W. D., BISHOP F. C., LOJENS M., SCHOONMAKER J. and WOLLAST R. (1983) Magnesian calcites: low-temperature occurrence, solubility and solid solution behavior. In *Carbonates: Mineralogy and Chemistry* (ed. R. J. REEDER), Chap. 4, pp. 97–144. *Reviews in Mineralogy*, **11**.
- MORSE J. W. (1974) Dissolution kinetics of calcium carbonate in sea water. III A new method for the study of carbonate reaction kinetics. *Amer. J. Sci.* **274**, 97–107.

- MORSE J. W. (1983) The kinetics of calcium carbonate dissolution and precipitation. In *Carbonates: Mineralogy and Chemistry* (ed. R. J. REEDER), Chap. 7, pp. 227–264. *Reviews in Mineralogy*, **11**.
- PALMER D. A. and VAN ELDIK R. (1983) The chemistry of metal carbonato and carbon dioxide complexes. *Chem. Rev.* **83**, 651–731.
- PERKINS E. H. and GUNTER W. D. (1989) Applications of SOLMINEQ.88 and SOLMINEQ.88 PC/SHELL to thermally enhanced oil recovery. *Fourth UNITAR/UNDP International Conference on Heavy Crude and Tar Sands Proceedings* (eds. R. F. Myer and E. J. Wiggins), Vol. 3, p. 413–422.
- PLUMMER L. N. and BUSENBERG E. (1982) The solubilities of calcite, aragonite and vaterite in the CO₂-H₂O solutions between 0 and 90°C, and an evaluation of the aqueous model for the system CaCO₃-CO₂-H₂O. *Geochim. Cosmochim. Acta* **46**, 1011–1040.
- PLUMMER L. N., WIGLEY T. M. L. and PARKHURST D. L. (1978) The kinetics of calcite dissolution in CO₂-water systems at 5° to 60°C and 0.0 to 1.0 atm CO₂. *Amer. J. Sci.* **278**, 179–216.
- PLUMMER L. N., PARKHURST D. L. and WIGLEY T. M. L. (1979) Critical review of the kinetics of calcite dissolution and precipitation. In *Chemical Modeling in Aqueous Systems. Speciation, Sorption, Solubility, and Kinetics* (ed. E. A. JENNE) pp. 537–573. *Amer. Chem. Soc. Symposium Series* **93**.
- POSEY-DOWTY J., CRERAR D., HELLMAN R. and CHANG C. (1986) Kinetics of mineral water reactions: theory, design and application of circulating hydrothermal equipment. *Amer. Miner.* **71**, 85–94.
- RICKARD D. and SJÖBERG E. L. (1983) Mixed control of calcite dissolution rates. *Amer. J. Sci.* **283**, 815–830.
- RIMSTIDT J. D. and BARNES H. L. (1980) The kinetics of silica-water reactions. *Geochim. Cosmochim. Acta* **44**, 1683–1699.
- RIMSTIDT J. D. and DOVE P. M. (1986) Mineral/solution reaction rates in a mixed flow reactor; wollastonite hydrolysis. *Geochim. Cosmochim. Acta* **50**, 2509–2516.
- SCHOTT J., BRANTLEY S., CRERAR D., GUY C., BORCSIK M. and CHRISTIAN W. (1989) Dissolution of strained calcite. *Geochim. Cosmochim. Acta* **53**, 373–382.
- SHARP W. E. and KENNEDY G. C. (1965) The system CaO-CO₂-H₂O in the two phase region calcite and aqueous solution. *J. Geol.* **73**, 391–403.
- WOOD B. J. and WALTHER J. V. (1983) Rates of hydrothermal reactions. *Science* **222**, 413–415.
- WOOD J. R. (1986) Thermal mass transfer in systems containing quartz and calcite. In *Roles of Organic Matter in Sediment Diagenesis* (ed. D. L. GAUTIER) pp. 169–180. SEPM Special Publication 38.

APPENDIX A

The raw data from the runs described in the text is given in the following tables. The values for the cations are all from ICP analysis, pH and C_q are the pH and the TIC of the quenched sample and C is the TIC of the basified sample, corrected for dilution with NaOH. The units of concentration are ppm. The last sample of each run is, unless otherwise noted, a standard of 26 ppm Ca. Those entries marked — were not analyzed and those listed as *nd* were below detection.

Table A.1. Raw data from experiments

Run	Sample	Time (hrs.)	Ca	C	Fe	Mg	pH	C _q
W130587	1	0.0	1.4	380.	3.4	<i>nd</i>	4.39	230.
	3	0.5	3.0	387.	1.7	<i>nd</i>	4.48	238.
	5	1.5	6.6	395.	0.9	<i>nd</i>	4.56	243.
	7	3.5	11.2	384.	0.5	0.1	4.83	213.
	9	7.5	16.7	385.	0.4	0.1	4.83	230.
	11	15.5	20.0	381.	0.4	0.2	4.76	217.
	13	31.5	21.2	391.	0.4	0.1	4.80	234.
	15	55.5	21.4	381.	0.4	0.3	4.79	224.
	17	79.5	21.0	375.	0.4	0.2	4.85	216.
	19	101.0	21.0	388.	0.6	<i>nd</i>	4.81	246.
	21	—	28.4	—	<i>nd</i>	3.1	—	—
W150987	1	0.0	1.4	475.	3.0	0.5	4.53	170.
	3	0.5	3.3	450.	0.6	0.2	4.67	118.
	5	1.5	7.5	448.	0.6	0.2	4.97	110.
	7	3.5	13.1	443.	0.5	0.3	5.28	92.
	9	6.5	17.6	448.	0.3	0.2	5.27	95.
	11	14.0	21.8	441.	0.3	0.3	5.47	99.
	13	31.0	21.6	454.	0.2	0.2	5.14	181.
	15	57.0	22.2	426.	0.3	0.2	5.22	170.
	17	81.3	21.8	450.	0.3	0.3	5.39	115.
	21	—	27.8	—	<i>nd</i>	3.1	—	—
	W271087	1	0.0	0.7	464.	0.1	0.3	4.54
3		0.5	3.6	458.	0.6	0.1	4.49	204.
5		1.5	8.0	466.	0.5	0.2	4.72	191.
7		3.5	12.4	474.	0.5	0.2	4.89	178.
9		7.0	17.4	488.	0.5	0.2	5.19	139.
11		15.0	20.2	471.	0.4	0.2	5.08	181.
13		31.0	21.4	472.	0.2	0.2	5.04	205.
15		130.4	21.4	284.	0.2	0.3	5.24	187.
18		—	26.8	—	<i>nd</i>	3.0	—	—

Table A.1. (Continued)

Run	Sample	Time (hrs.)	Ca	C	Fe	Mg	pH	Cl ^e
W251088	1	0.0	2.2	85.	<i>nd</i>	0.2	—	—
	3	0.5	6.5	88.	<i>nd</i>	0.1	—	—
	5	1.0	11.9	91.	<i>nd</i>	<i>nd</i>	—	—
	7	2.0	19.8	96.	<i>nd</i>	0.1	—	—
	9	3.5	26.4	110.	<i>nd</i>	<i>nd</i>	—	—
	11	8.0	33.4	95.	<i>nd</i>	0.2	—	—
	13	15.0	35.6	104.	<i>nd</i>	0.2	—	—
	15	35.0	37.2	96.	<i>nd</i>	0.3	—	—
	17	52.0	36.8	—	<i>nd</i>	0.3	—	—
W141288	19	—	23.6	—	<i>nd</i>	0.2	—	—
	2	0.0	1.2	87.	0.1	0.5	—	—
	4	0.5	6.6	77.	<i>nd</i>	0.3	—	—
	6	1.0	9.6	79.	<i>nd</i>	0.1	—	—
	8	2.0	17.9	83.	<i>nd</i>	0.3	—	—
	10	3.5	24.4	84.	<i>nd</i>	0.3	—	—
	12	7.5	30.4	87.	<i>nd</i>	<i>nd</i>	—	—
	14	14.7	34.8	91.	<i>nd</i>	0.3	—	—
	16	37.2	34.6	87.	0.2	0.3	—	—
W020389	18	61.8	36.4	90.	<i>nd</i>	0.3	—	—
	—	—	—	—	—	—	—	—
	2 ^d	0.0	3.4	0.5	0.1	0.1	8.4	—
	4	0.5	1.1	0.7	0.1	<i>nd</i>	8.7	—
	6	1.0	2.0	1.2	0.1	<i>nd</i>	6.3	—
	8	2.0	2.9	1.3	0.1	0.2	7.3	—
	10	4.0	4.4	1.8	0.1	<i>nd</i>	7.6	—
	12	7.0	5.1	2.1	0.1	0.1	8.6	—
	14	12.0	5.9	2.4	<i>nd</i>	<i>nd</i>	8.8	—
	16	20.0	6.1	2.5	0.1	<i>nd</i>	9.0	—
	18	45.0	6.5	2.6	0.1	0.1	9.2	—
W200389	20	91.0	6.7	3.5	<i>nd</i>	<i>nd</i>	9.0	—
	22	—	27.0	—	<i>nd</i>	3.0	—	—
	2	0.0	1.8	195.	0.2	0.2	—	—
	4	0.5	8.1	200.	<i>nd</i>	<i>nd</i>	—	—
	6	1.0	14.6	194.	<i>nd</i>	<i>nd</i>	—	—
	8	2.0	24.4	200.	0.3	<i>nd</i>	—	—
	10	4.0	43.6	208.	<i>nd</i>	0.1	—	—
	12	7.0	63.0	238.	0.1	0.2	—	—
	14	12.7	86.5	203.	<i>nd</i>	0.1	—	—
	16	37.2	106.5	213.	<i>nd</i>	0.1	—	—
	18	46.0	108.0	214.	<i>nd</i>	<i>nd</i>	—	—
W040489	20	69.0	109.0	207.	<i>nd</i>	0.2	—	—
	22	—	29.6	—	<i>nd</i>	3.4	—	—
	2	0.0	4.7	0.	0.4	0.4	—	70.9
	4	0.5	19.0	1.	0.7	0.2	—	69.1
	6	1.0	27.2	1.	0.9	0.1	—	67.4
	8	1.5	32.0	2.	0.8	0.1	—	65.7
	10	2.5	35.8	7.	0.5	<i>nd</i>	—	64.1
	12	4.0	39.8	10.	0.2	<i>nd</i>	—	62.5
	14	6.5	42.0	11.	0.3	<i>nd</i>	—	60.9
	16	15.5	44.2	12.	0.4	0.3	—	59.4
	18	38.8	49.4	12.	0.3	0.1	—	57.9
20	69.0	48.0	—	0.2	0.2	—	56.5	
22	—	28.6	—	<i>nd</i>	3.7	—	—	

^a Sample froze, CO₂ loss likely.

^b Water from infill lines.

^c milliQ water.

^d Sample contaminated.

^e From HCl, assumed to decrease by 2.5% with each sample.

